



Synthesis, characterization of the phenylquinoline-based on iridium(III) complexes for solution processable phosphorescent organic light-emitting diodes

Juhyeon Park^a, Jin Su Park^a, Young Geun Park^b, Jin Yong Lee^b, Jae Wook Kang^c, Jun Liu^d, Liming Dai^d, Sung-Ho Jin^{a,*}

^a Department of Chemistry Education, Graduate Department of Materials Chemistry, Institute for Plastic Information and Energy Materials, Pusan National University, Busan 609-735, Republic of Korea

^b Department of Chemistry, Sungkyunkwan University, Suwon 440-746, Republic of Korea

^c Department of Flexible and Printable Electronics, Chonbuk National University, Jeonju 561-756, Republic of Korea

^d Department of Macromolecular Science and Engineering, Case Western Reserve University, 10900 Euclid Avenue, Cleveland, OH 44106, United States

ARTICLE INFO

Article history:

Received 27 November 2012

Received in revised form 8 May 2013

Accepted 9 May 2013

Available online 23 May 2013

Keywords:

Organic light-emitting diodes

Iridium complex

Phosphorescent

Solution processable

Picolinic acid N-oxide

ABSTRACT

A new series of highly efficient Ir(III) complexes, (DPQ)₂Ir(pic-N-O), (F₄PPQ)₂Ir(pic-N-O), (FPQ)₂Ir(pic-N-O), and (CPQ)₂Ir(pic-N-O) were synthesized for phosphorescent organic light-emitting diodes (PhOLEDs), and their photophysical, electrochemical, and electroluminescent (EL) properties were investigated. The Ir(III) complexes, including picolinic acid N-oxide (pic-N-O) ancillary ligand, are comprised with the various main ligands such as 2,4-diphenylquinoline (DPQ), 4-phenyl-2-(2,3,4,5-tetrafluorophenyl)quinoline (F₄PPQ), 2-(9,9-diethyl-9H-fluoren-2-yl)-4-phenylquinoline (FPQ) and 9-ethyl-3-(4-phenylquinolin-2-yl)-9H-carbazole. Remarkably, high performance PhOLEDs using a solution-processable (DPQ)₂Ir(pic-N-O) doped CBP host emission layer were fabricated to give a high luminance efficiency (LE) of 26.9 cd/A, equivalent to an external quantum efficiency (EQE) of 14.2%.

The calculated HOMO–LUMO energy gaps for (DPQ)₂Ir(pic-N-O), (F₄PPQ)₂Ir(pic-N-O), (FPQ)₂Ir(pic-N-O) and (CPQ)₂Ir(pic-N-O) were in good agreement with the experimental results.

© 2013 Elsevier B.V. All rights reserved.

1. Introduction

Organic light-emitting diodes (OLEDs) are being most extensively researched for many applications, including flat-panel displays and solid-state lightings [1,2]. Internal quantum efficiencies near unity, corresponding to the harvesting of all singlet and triplet states, can be achieved in OLEDs composed of phosphorescent complexes based on ligated iridium (Ir), platinum, ruthenium, and osmium. As of now available light-emitting materials, phosphorescent iridium (Ir) complexes are particularly promising because

they can emit the light from both singlet and triplet excitons, enabling the fabrication of phosphorescent organic light-emitting diodes (PhOLEDs) with close to 100% internal quantum efficiency [3,4]. The efficiencies, brightness, and wavelength emissions of Ir(III) complexes strongly depend on the molecular structure of a cyclometalated ligand. The emission wavelength of Ir(III) complexes normally can be altered by changing the electron density or position of substituents on the main ligands. For example, emission wavelengths of these Ir(III) complexes can be adjusted to cover the entire visible spectral region by modifying or varying cyclometalated 2-arylpyridine ligands [5–7]. For example, the emission wavelength of Ir(III) complexes can be tuned to cover the

* Corresponding author.

E-mail address: shjin@pusan.ac.kr (S.-H. Jin).

whole visible region by modification or variation of cyclometalated 2-arylpyridine main ligands and ancillary ligands [8]. Therefore, the design and preparation of novel cyclometalated ligands for Ir(III) complexes has attracted great attention.

The most well-known fabrication strategies for the PhOLEDs are thermal evaporation and solution processing methods. The thermal deposition enables the formation of complicated multilayer device architectures for excellent device performance with high efficiencies [9,10]. However, it is not easy to form the multistacked layers of organic materials by the solution processing method since the solvent used for depositing organic materials usually causes unwanted swelling and/or damage to the previously coated layers [11]. For this reason, the performance of PhOLEDs based on the thermally evaporated thin films is generally better than that of the solution processed PhOLEDs. Apart from the above-mentioned limitation, however, the solution processing has several advantages, including its simplicity, manufacture ability on a large scaled area, extremely low-cost, and can be extended to large area substrates, and to high-throughput reel-to-reel processing [12–14]. Additionally, it is possible to realize co-doping of several dopants by mixing the dopants and host material in solution. Thus, many research groups are still focused on the synthesis of suitable materials for the solution fabrication processes to improve the device performance [15]. At CES 2013 Panasonic unveiled a 56" 4K (3840 × 2160) OLED TV panel prototype that was produced using an all printing method.

The majority of PhOLEDs based on solution processed layers contain oligomers, conjugated polymers [16–20] and more recently dendrimers [21–24]. There have been various approaches to develop high efficiency solution processed PhOLEDs. The most widely used method was to use a mixed polymeric host doped with a phosphorescent dopant. Poly(N-vinylcarbazole) (PVK) has typically been used as the hole transport type host material for solution processed PhOLEDs and several electron transport type host materials were mixed with the PVK host material. A high quantum efficiency above 15% has been achieved in PVK based PhOLEDs [25,26]. High molecular-weight materials that cannot be vapor-deposited, such as polymers or oligomers, can show relatively good morphological stability relative to small molecules. One drawback with solution processing, at least of high molecular weight materials, is that it is generally more difficult to purify these materials; high material purity is considered to be a critical factor in achieving long-lived devices. Careful design of materials can help circumvent this problem.

We have previously reported the synthesis and characterization of highly efficient red Ir(III) complexes by making use of carbazole substituted phenylquinoline (CPQ) moieties as a main ligands [27]. Further to our previous work, we report here the synthesis, redox, photophysical, and electroluminescent (EL) properties of novel heteroleptic Ir(III) complexes using phenyl, perfluorinated phenyl, or fluorenyl substituted phenylquinoline-based main ligands (DPQ, F₄PPQ, and FPQ) and picolinic acid N-oxide (pic-N-O) as an ancillary ligand for solution processing of the emitting layer in PhOLEDs. Solution processable PhOLEDs

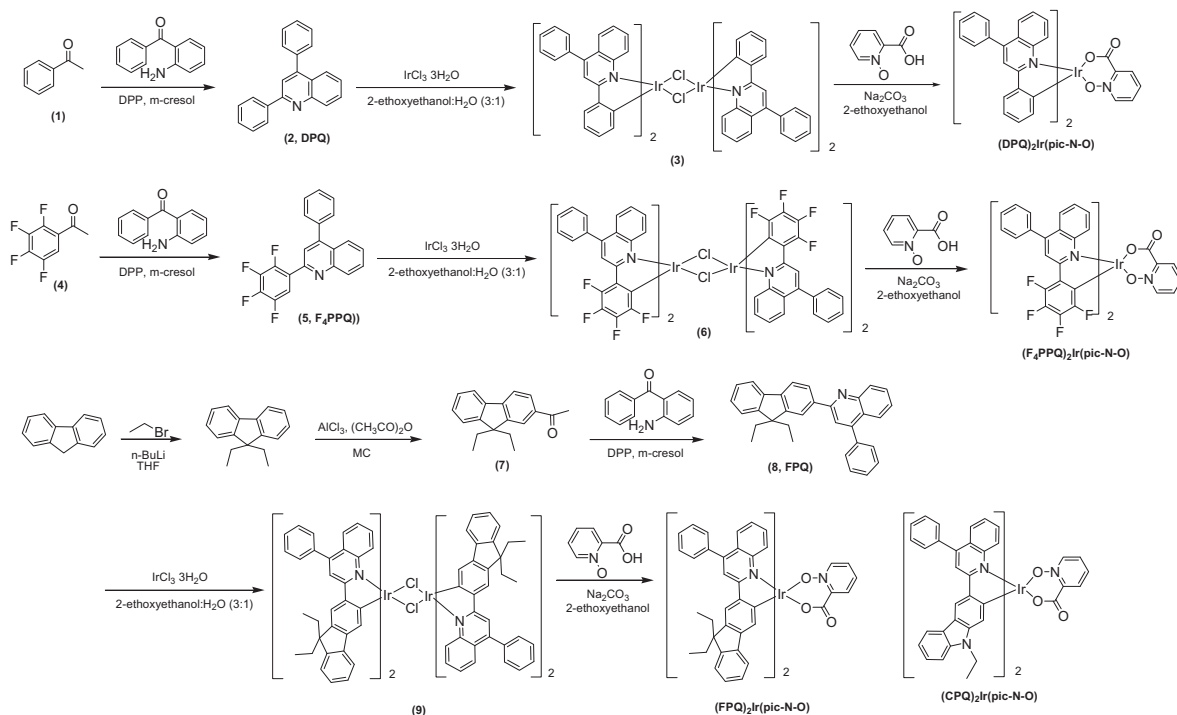
fabricated using these Ir(III) complexes exhibit a maximum external quantum efficiency of 14.2% with the Commission Internationale de l'Eclairage (CIE) coordinates of (0.600, 0.397).

2. Results and discussion

Three novel phenylquinoline (PQ) derived main ligands, 2,4-diphenylquinoline (DPQ) (2), 4-phenyl-2-(2,3,4,5-tetrafluorophenyl)quinoline (F₄PPQ) (5), and 2-(9,9-diethyl-9H-fluoren-2-yl)-4-phenylquinoline (FPQ) (8) were synthesized by an acid-catalyzed Friedlander condensation reaction [28,29]. (CPQ)₂Ir(pic-N-O) was synthesized according to our previously reported literature [27]. Condensation of starting materials (1, 4, 7) with 2-aminobenzophenone gave the desired donor-acceptor type of PQ derivatives (2, 5, 8) in over 75% yield. Cyclometalated Ir(III) μ -chloride bridged dimers (3, 6, 9) were synthesized by iridium trichloride hydrate with a 2.5 equivalents of main ligands (2, 5, 8) developed in our own laboratories. The above dimers can be easily converted into heteroleptic Ir(III) complexes by replacing of the two bridge chlorides with bidentate monoanionic ancillary ligands. The Ir(III) complexes were prepared by three dimers with the pic-N-O ancillary ligand as shown in Scheme 1. The resulting Ir(III) complexes were mainly focused on the modification of PQ-based main ligands such as DPQ, F₄PPQ, and FPQ, which tuned the electro-optical properties and emission colors of Ir(III) complexes. Subsequently, the four Ir(III) complexes, [(2,4-diphenylquinoline)₂Iridium picolinic acid N-oxide [(DPQ)₂Ir(pic-N-O)], [4-phenyl-2-(2,3,4,5-tetrafluorophenyl)quinoline]₂Iridium picolinic acid N-oxide [(F₄PPQ)₂Ir(pic-N-O)], [2-(9,9-diethyl-9H-fluoren-2-yl)-4-phenylquinoline]₂Iridium picolinic acid N-oxide [(FPQ)₂Ir(pic-N-O)], and [9-ethyl-3-(4-phenylquinolin-2-yl)-9H-carbazole]₂Iridium picolinic acid N-oxide [(CPQ)₂Ir(pic-N-O)], were purified with the silica gel column and their structures and purities were characterized using ¹H-, ¹³C-NMR, HPLC, elemental analysis, HR-MS, differential scanning calorimetry (DSC), thermal gravimetric analysis (TGA), cyclic voltammetry (CV), UV-visible, and photoluminescent (PL) spectroscopy.

Thermal stability of the Ir(III) complexes was evaluated using TGA (Fig. 1) and DSC under a nitrogen atmosphere with the 5% weight loss temperatures ($\Delta T_{5\%}$) and other results being summarized in Table 1. The TGA curves given in Fig. 1 indicated that all the Ir(III) complexes showed excellent thermal stability with their $\Delta T_{5\%}$ within the range of 361–380 °C while the glass transition temperature (T_g) of these Ir(III) complexes were found to be in the range of 180–287 °C (Table 1). The thermal stability of (CPQ)₂Ir(pic-N-O) is higher than that of (DPQ)₂Ir(pic-N-O), (F₄PPQ)₂Ir(pic-N-O), and (FPQ)₂Ir(pic-N-O). The good thermal stabilities observed for all of the newly synthesized Ir(III) complexes indicate that they will not be easily distorted even under high temperatures associated with heat generation during the operation of PhOLEDs, leading to long device lifetimes.

Fig. 2 presents the UV-visible absorption and emission spectra of the Ir(III) complexes in chloroform solution. As



Scheme 1. Synthetic routes of main ligands and their Ir(III) complexes.

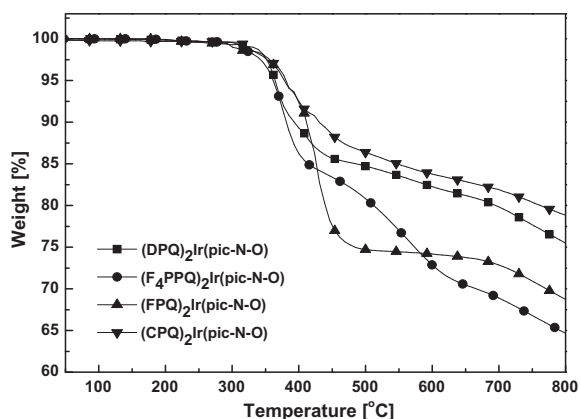


Fig. 1. TGA trace of Ir(III) complexes measured at a scan rate of 10 °C/min under N₂ atmosphere.

shown in Fig. 2a, the absorption bands are observed in the range of 280–550 nm. The intense peaks in the UV region below 400 nm were assigned to the allowed $^1\pi-\pi^*$ transitions of the C₆N ligands. The weaker absorption tails that appeared above 400 nm were assigned to singlet and triplet transitions of MLCT. In the UV–visible absorption spectra for (DPQ)₂Ir(pic-N-O) and (CPQ)₂Ir(pic-N-O), two MLCT bands are clearly separated at 409 (41,500 M⁻¹cm⁻¹) and 467 nm (39,700 M⁻¹cm⁻¹) for (DPQ)₂Ir(pic-N-O) and at 410 (46,200 M⁻¹cm⁻¹) and 481 nm (40,400 M⁻¹cm⁻¹) for (CPQ)₂Ir(pic-N-O), respectively. The spin forbidden 3 MLCT at 467 nm for (DPQ)₂Ir(pic-N-O) and 481 nm for

(CPQ)₂Ir(pic-N-O) have intensity by mixing with the higher lying 1 MLCT transition through the strong spin–orbital coupling of Ir(III) complexes [30]. In the case of (F₄PPQ)₂Ir(pic-N-O) and (FPQ)₂Ir(pic-N-O), they are not separated with a broad band at 410–480 nm for (F₄PPQ)₂Ir(pic-N-O) and at 450–550 nm for (FPQ)₂Ir(pic-N-O).

Under photoexcitation, all the Ir(III) complexes tuned the emission colors from orange-red to red light as shown in Fig. 2b, which originated from the predominantly ligand-centered $^3\pi-\pi^*$ excited state in the solution state. The maximum emission peaks of (DPQ)₂Ir(pic-N-O), (F₄PPQ)₂Ir(pic-N-O), (FPQ)₂Ir(pic-N-O), and (CPQ)₂Ir(pic-N-O) are shown at 586, 569, 610, and 599 nm, respectively. Due to the introduction of electron acceptor perfluorinated phenyl group in (F₄PPQ)₂Ir(pic-N-O), the PL spectrum is blue shifted compared to (DPQ)₂Ir(pic-N-O). On the other hand, the emission spectra of (FPQ)₂Ir(pic-N-O) and (CPQ)₂Ir(pic-N-O) complexes show a bathochromic shift due to an increased conjugation length and more electron donating fluorenyl and carbazolyl groups into the PQ-based main ligands. The PL spectra of Ir(III) complexes doped in poly(methyl methacrylate) film exhibit red shifts compared to those in the chloroform solution. The characteristics red shift around 10–20 nm of the PL spectra in the film state are thought to be related to the formation of intermolecular aggregation. Another important requirement for PhOLED applications is that the Ir(III) complexes should have high PL quantum efficiencies (Φ_{pl}). The Φ_{pl} of Ir(III) complexes in chloroform solution were measured with (piq)₂Ir(acac) as a standard ($\Phi_{\text{pl}} = 0.2$). The Φ_{pl} for (DPQ)₂Ir(pic-N-O), (F₄PPQ)₂Ir(pic-N-O), (FPQ)₂Ir(pic-N-O), and

Table 1
Photophysical, electrochemical and thermal data for Ir(III) complexes.

Compound	T_d ($^{\circ}\text{C}$) ^a	T_g ($^{\circ}\text{C}$) ^b	λ_{abs} (log ϵ (nm)) ^c	λ_{em} (nm) ^d	λ_{em} (nm) ^e	Φ_{pl} (%) ^f	HOMO/LUMO (eV) ^g
(DPQ) ₂ Ir(pic-N-O)	364	245	280 (4.94), 349 (4.63), 409 (4.15), 467 (3.97)	586	605	0.83	−5.5/−3.2
(F ₄ PPQ) ₂ Ir(pic-N-O)	361	180	288 (5.30), 349 (4.48), 440 (3.66)	569	575	0.67	−5.8/−3.3
(FPQ) ₂ Ir(pic-N-O)	378	265	324 (4.82), 372 (4.77), 489 (3.96)	610	619	0.50	−5.5/−3.3
(CPQ) ₂ Ir(pic-N-O)	380	287	316 (5.07), 374 (4.86), 410 (4.62), 481 (4.04)	599	619	0.76	−5.3/−3.1

^a Temperature with 5% mass loss measure by TGA with a heating rate of 10 $^{\circ}\text{C}/\text{min}$ under N_2 .

^b Glass transition temperature determined by DSC with a heating rate of 10 $^{\circ}\text{C}/\text{min}$ under N_2 .

^c Measured in CHCl_3 solution at 1×10^{-5} M concentration.

^d Maximum emission wavelength measured in CHCl_3 solution at 1×10^{-5} M concentration.

^e Maximum emission wavelength measured in film state onto quartz glass.

^f Measured in 1×10^{-5} M CHCl_3 solution relative to (pic)₂Ir(acac) ($\Phi_{\text{pl}} = 0.2$) with 371 nm excitation.

^g Determined from the onset of CV oxidation and UV–visible absorption edge.

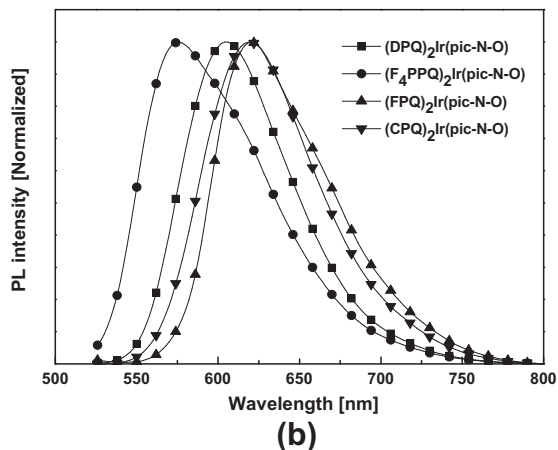
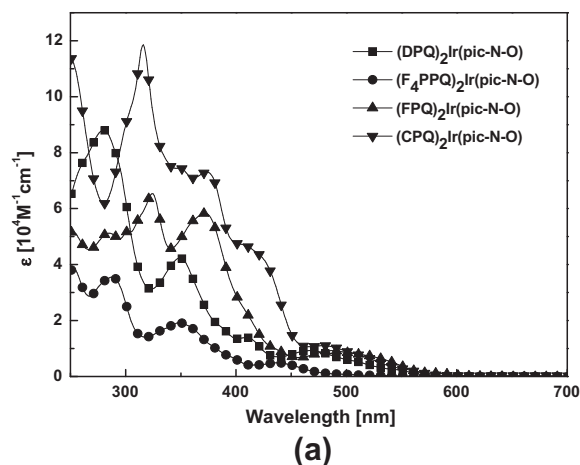


Fig. 2. Electronic absorption (a) and PL (b) spectra of Ir(III) complexes in CHCl_3 solution.

(CPQ)₂Ir(pic-N-O) were found to be 0.83, 0.67, 0.50, and 0.76, respectively, with (DPQ)₂Ir(pic-N-O) showing a higher PL quantum yield than that of other Ir(III) complexes. The high Φ_{pl} for (DPQ)₂Ir(pic-N-O) is well correlated with the higher PhOLED performance than that of (F₄PPQ)₂Ir(pic-N-O), (FPQ)₂Ir(pic-N-O), and (CPQ)₂Ir(pic-N-O) (*vide*

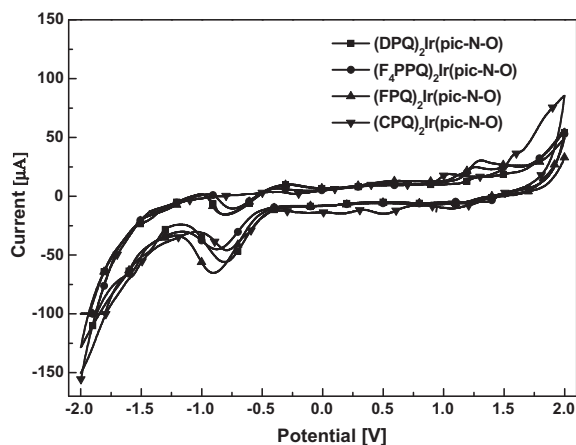


Fig. 3. Cyclic voltammograms of Ir(III) complexes.

infra). The photophysical properties of the Ir(III) complexes are also summarized in Table 1.

To investigate the charge carrier injection properties of the Ir(III) complexes and evaluate their highest occupied molecular orbital (HOMO) and lowest unoccupied molecular orbital (LUMO) energy levels, we carried out redox measurements using CV. The Ir(III) complexes were designed on the basis of considerations that the possibility to tune HOMO–LUMO energy gaps by modification of electron donor and acceptor substituents at PQ-based main ligands. By introducing of PQ moiety as a n-type semiconductor and phenyl, perfluorinated phenyl, fluorenyl, and carbazolyl units as a p-type semiconductor, all the Ir(III) complexes showed a reversible redox process over the anodic and cathodic range, suggesting that these Ir(III) complexes stabilized the formation of both cation and anion radicals in PhOLEDs, as shown in Fig. 3. The HOMO energy levels of (DPQ)₂Ir(pic-N-O), (F₄PPQ)₂Ir(pic-N-O), (FPQ)₂Ir(pic-N-O), and (CPQ)₂Ir(pic-N-O) with respect to the ferrocene/ferrocenium (4.8 eV) standard were estimated to be −5.5, −5.8, −5.5, and −5.3 eV, respectively. The optical band gaps (E_g) of Ir(III) complexes were determined from the UV–visible absorption edge and found to be 2.3 eV for (DPQ)₂Ir(pic-N-O), 2.5 eV for (F₄PPQ)₂Ir(pic-N-O), 2.2 eV for (FPQ)₂Ir(pic-N-O) and (CPQ)₂Ir(pic-N-O).

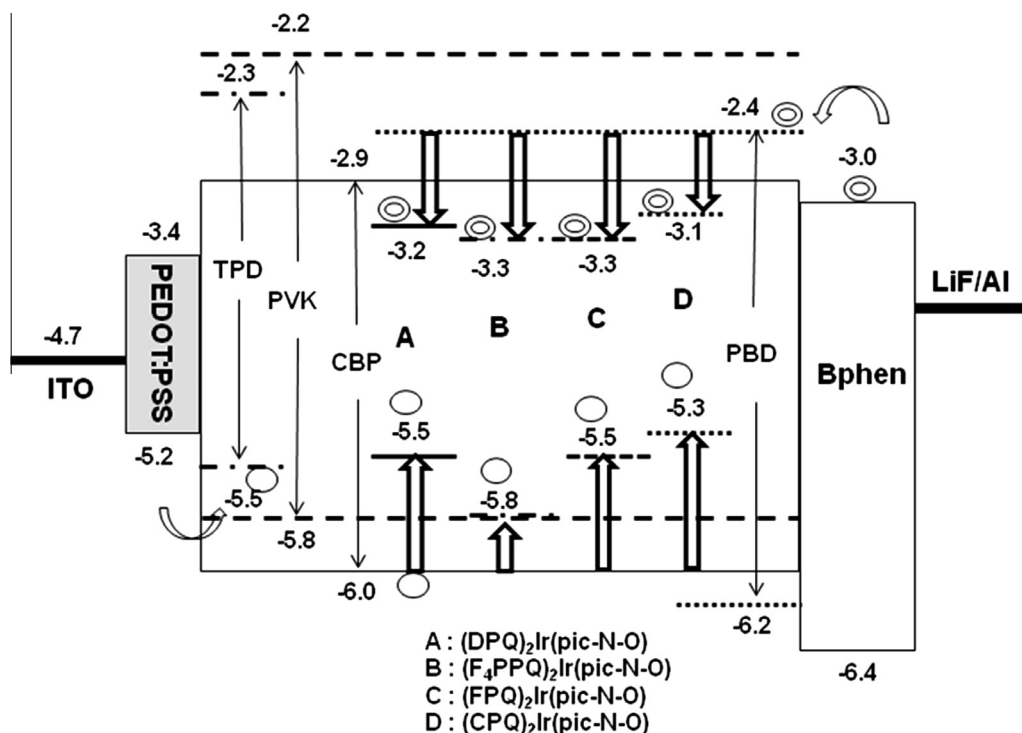


Fig. 4. Structure of the PhOLEDs and energy levels of the materials used in this study.

From the above observation, we found that the introduction of electron accepting perfluorinated phenyl group into the PQ-based main ligand, the Ir(III) complex possesses a higher energy band gap than that of other Ir(III) complexes with electron donor based main ligands. The LUMO energy levels were calculated from the values of the E_g and HOMO energies to be -3.1 eV for (CPQ)₂Ir(pic-N-O), -3.2 eV for (DPQ)₂Ir(pic-N-O), and -3.3 eV for (F₄PPQ)₂Ir(pic-N-O) and (FPQ)₂Ir(pic-N-O). The HOMO and LUMO energy levels data were also summarized in Table 1.

To evaluate the EL properties of these Ir(III) complexes, solution processed PhOLEDs were fabricated using (DPQ)₂Ir(pic-N-O), (F₄PPQ)₂Ir(pic-N-O), (FPQ)₂Ir(pic-N-O), and (CPQ)₂Ir(pic-N-O) as a dopant in the emitting layer (EML). The PhOLEDs consisted of multilayer films with a configuration of ITO/PEDOT:PSS (40 nm)/EML (70 nm)/Bphen (20 nm)/LiF (0.7 nm)/Al (100 nm) as shown in Fig. 4. The Ir(III) complexes were doped into 4,4'-bis(9-cabazoyl)biphenyl (CBP) [or poly(N-vinylcarbazole) (PVK)], hole-transporting N,N'-diphenyl-N,N'-bis(3-methyl-phenyl)-[1,1'-biphenyl]-4,4'-diamine (TPD), and electron-transporting 2-(4-biphenyl)-5-(4-tert-butylphenyl)-1,3,4-oxadizole (PBD), (56:12:24) as an EML at a concentration of 8 wt%, and then the EML solution was spin-coated with chlorobenzene to give a 70 nm thick film. Due to the amorphous nature of these Ir(III) complexes, they all possessed very good film forming properties and good chemical compatibility with the CBP (or PVK), TPD, and PBD as a host component, resulting in a homogeneous distribution of Ir(III) complexes in the EML. 4,7-Diphenyl-1,10-phenanthroline (Bphen) was thermally evaporated at a base

pressure of 6×10^{-6} Torr on the spin-coated EML as an electron transport layer as well as hole blocking layer due to the high electron mobility (2.8×10^{-4} cm²/V s) and high-lying HOMO [11].

Fig. 5 shows the surface morphology of the spin coated films of the EML. By replacing PVK with CBP as the host matrix reduces the surface roughness of EML. During the spin coating, the films formed by small molecules and polymers show different degree of phase separation [11,31,32]. The better uniformity of the CBP-based EML may be partially responsible for the better device performance (*vide infra*).

The energy level diagram shows that the HOMO and LUMO energy levels of Ir(III) complexes lie above and below those of CBP (or PVK) host, respectively. Therefore, it is expected that Ir(III) complexes trap both electrons and holes within EML. Moreover, the hole block/electron transporting properties of PBD was introduced into the host components for effective electron injection/transport and charge carrier balance within the EML. The LUMO energy levels of PBD and Bphen were closely aligned to the LUMO levels of Ir(III) complexes. This good alignment of energy levels is important for efficient electron injection into the both transport molecules and Ir(III) complexes.

Fig. 6 presents the current density–voltage–luminance (J – V – L) characteristics and the luminance efficiency (LE) and power efficiency (PE) as a function of current density of CBP-based PhOLEDs using four types of Ir(III) complexes as a dopant. The performance of PhOLEDs and EL emission characteristics are summarized in Table 2. The CBP-based PhOLEDs show turn-on voltages of 4.5–6 V; these values are lower than those of PVK-based PhOLEDs. The turn-on

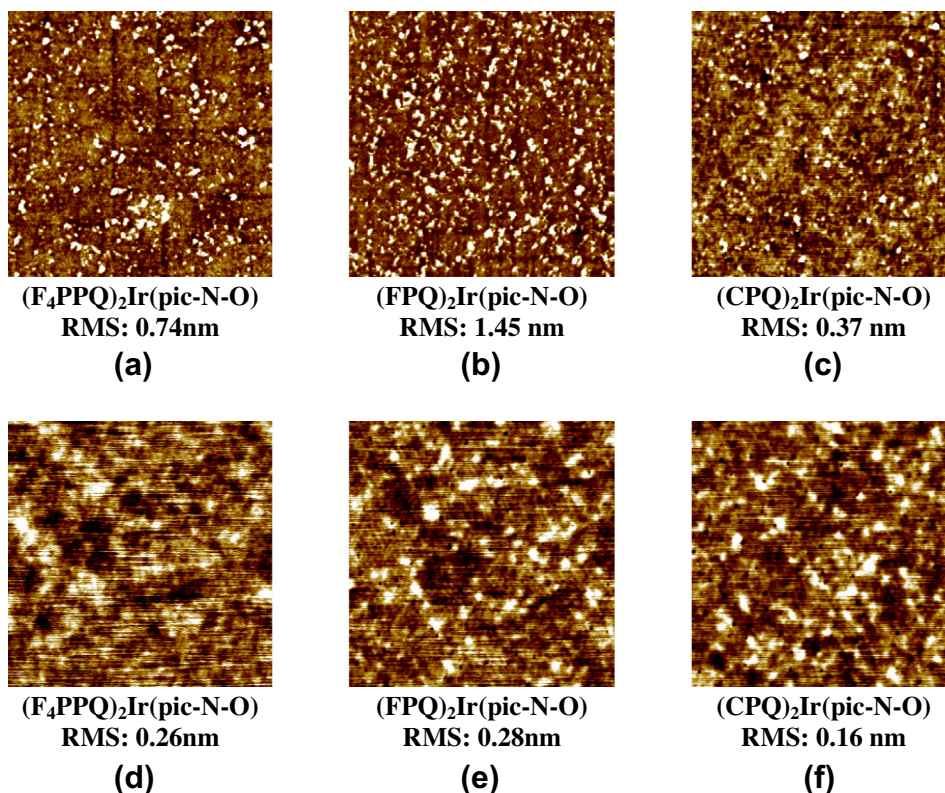


Fig. 5. AFM images of thin film formed by spin coating (a) PVK:TPD:PBD:(F₄PPQ)₂Ir(pic-N-O), (b) PVK:TPD:PBD:(FPQ)₂Ir(pic-N-O), (c) PVK:TPD:PBD:(CPQ)₂Ir(pic-N-O), (d) CBP:TPD:PBD:(F₄PPQ)₂Ir(pic-N-O), (e) CBP:TPD:PBD:(FPQ)₂Ir(pic-N-O) and (f) CBP:TPD:PBD:(CPQ)₂Ir(pic-N-O).

voltage of PVK host devices is higher than that of CBP host, and the current density is lower in comparison to CBP host. This clearly demonstrates a reduced conductivity of PVK host devices. The higher conductivity and higher efficiencies of CBP host devices are probably due to the much higher hole mobility of CBP ($\mu_h \sim 10^{-3} \text{ cm}^2/\text{Vs}$) than of PVK ($\mu_h \sim 10^{-9} \text{ cm}^2/\text{Vs}$), but may also be related to the smoother surface of the CBP-based layer [11].

The external quantum efficiencies (EQEs) of the Ir(III) complexes as a function of luminance are depicted in Fig. 7. With increasing luminance, the EQE of Ir(III) complexes decreased slightly. Among the Ir(III) complexes, (DPQ)₂Ir(pic-N-O) exhibited the highest PhOLED performance, showing a maximum EQE of 14.2%, LE of 26.9 cd/A, and PE of 12.1 lm/W, with a maximum brightness of 14,070 cd/m². However, the PVK-based PhOLED using (DPQ)₂Ir(pic-N-O) as a dopant showed a maximum EQE of 6.7%, LE of 12.5 cd/A, PE of 3.3 lm/W, and a maximum brightness of 9969 cd/m². The CBP-based PhOLEDs using (F₄PPQ)₂Ir(pic-N-O), (FPQ)₂Ir(pic-N-O), and (CPQ)₂Ir(pic-N-O) as a dopant showed notably improved device performance compared to the PVK-based PhOLEDs. The observed higher device performance for the CBP-based PhOLEDs can be attributed to the higher hole mobility of CBP ($1.0 \times 10^{-3} \text{ cm}^2/\text{Vs}$) than that of PVK ($4.8 \times 10^{-9} \text{ cm}^2/\text{Vs}$) [11,33,34].

Electroluminescent (EL) spectra of the CBP-based PhOLEDs are shown in Fig. 8. The EL spectra of all PhOLEDs were

almost identical to their PL spectra, indicating that EL and PL are from the same excited state. The absence of any emission peaks of CBP (or PVK), TPD and PBD indicated the effective charge trapping on the Ir(III) complexes and/or effective energy transfer to the Ir(III) complexes. The maximum emission peak of Ir(III) complexes are tuned by slight modification of main ligands, and the peak values observed for the PhOLEDs are in the order of (FPQ)₂Ir(pic-N-O) (615 nm) > (CPQ)₂Ir(pic-N-O) (608 nm) > (DPQ)₂Ir(pic-N-O) (597 nm) > (F₄PPQ)₂Ir(pic-N-O) (570 nm). The CIE coordinates of (DPQ)₂Ir(pic-N-O) was (0.600, 0.397) representing orange emission, (F₄PPQ)₂Ir(pic-N-O) (0.526, 0.469) representing yellowish orange emission, (FPQ)₂Ir(pic-N-O) (0.660, 0.338) and (CPQ)₂Ir(pic-N-O) (0.626, 0.372) representing red emission in the 1931 CIE diagram.

To gain an insight into the observed photo-physical properties of the Ir(III) complexes, density functional theory (DFT) calculations were performed by using the Becke's three parameterized Lee–Yang–Parr exchange functional (B3LYP) and a suite of Gaussian 09 programs [35]. The split valance 6–31G* basis sets were used except Ir(III) metal for which the Hay–Wadt effective core potential of a double zeta basis set (LANL2DZ) was used. The calculated Ir(III) complexes had very similar structures with octahedral geometry. The calculated HOMOs and LUMOs of (DPQ)₂Ir(pic-N-O), (F₄PPQ)₂Ir(pic-N-O), (FPQ)₂Ir(pic-N-O) and (CPQ)₂Ir(pic-N-O) are shown in Fig. 9. The delocalization of HOMOs in all complexes is very similar while that of

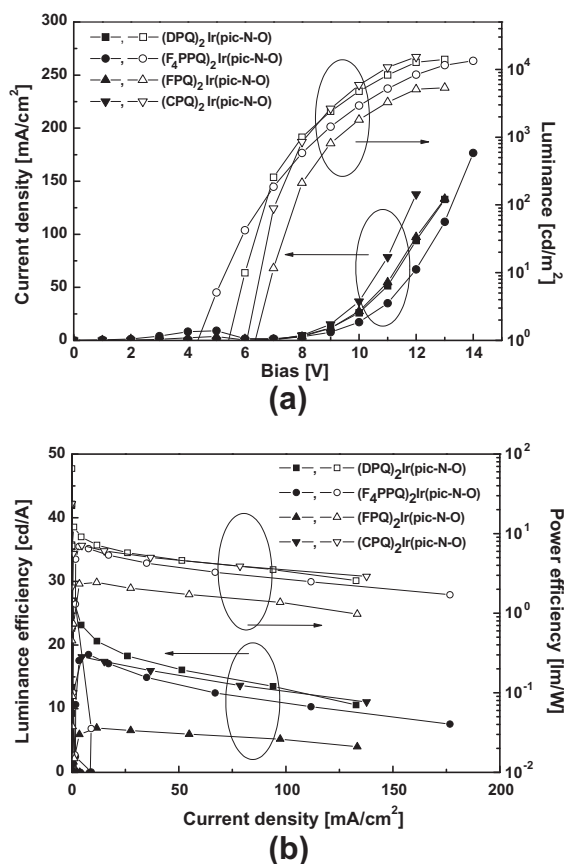


Fig. 6. (a) Current density–voltage–luminance and (b) luminance efficiency–current density–power efficiency characteristics.

LUMOs is slightly different. The HOMOs of all iridium complexes are mostly distributed over the iridium metal and one of the phenylquinoline moieties. However, the LUMOs of (F₄PPQ)₂Ir(pic-N-O) and (FPQ)₂Ir(pic-N-O) are mostly delocalized on the F₄PPQ and FPQ ligands, respectively, while those of (DPQ)₂Ir(pic-N-O) and (CPQ)₂Ir(pic-N-O) showed the delocalization of electron density over the pic-N-O ancillary ligands. These results indicated that the metal to ligand charge transfer (MLCT) can dominantly contribute to the transition property of (F₄PPQ)₂Ir(pic-N-O) and (FPQ)₂Ir(pic-N-O) while the transition properties

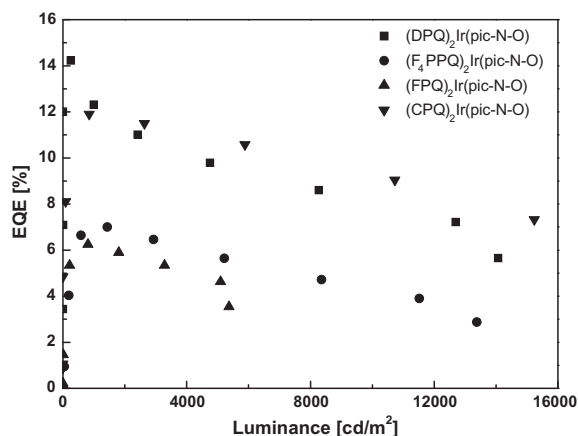


Fig. 7. External quantum efficiency–luminance characteristics.

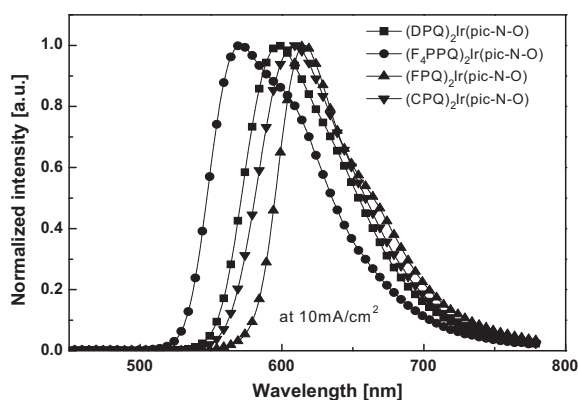


Fig. 8. EL spectra of Ir(III) complexes.

of (DPQ)₂Ir(pic-N-O) and (CPQ)₂Ir(pic-N-O) are attributed to ligand to ligand charge transfer (LLCT). The HOMO–LUMO energy gaps for (DPQ)₂Ir(pic-N-O), (F₄PPQ)₂Ir(pic-N-O), (FPQ)₂Ir(pic-N-O) and (CPQ)₂Ir(pic-N-O) were calculated to be 3.18, 3.34, 3.02 and 2.86 eV, which corresponded to the absorption wavelengths of 390, 372, 411 and 433 nm, respectively. These calculated results are in good agreement with the experimentally observed

Table 2

EL performance of PhOLEDs based on solution processed emitting layer.

Host	Dopant	V _{on} (V) ^a	V (V) ^b	EQE (%) ^c	LE (cd/A) ^c	PE (lm/W) ^c	LE (cd/m ²) ^c	CIE (x,y) ^d
CBP:TPD:PBD	(DPQ) ₂ Ir(pic-N-O)	5.1	8.0	14.2	26.9	12.1	14,070	0.600, 0.397
CBP:TPD:PBD	(F ₄ PPQ) ₂ Ir(pic-N-O)	4.5	8.6	7.0	18.5	6.9	13,380	0.526, 0.469
CBP:TPD:PBD	(FPQ) ₂ Ir(pic-N-O)	6	9.2	8.9	9.9	3.9	5238	0.660, 0.338
CBP:TPD:PBD	(CPQ) ₂ Ir(pic-N-O)	6	8.1	11.9	18.1	7.1	15,240	0.626, 0.372
PVK:TPD:PBD	(DPQ) ₂ Ir(pic-N-O)	8	12.2	6.7	12.5	3.3	9969	0.591, 0.357
PVK:TPD:PBD	(F ₄ PPQ) ₂ Ir(pic-N-O)	7.8	13.5	5.4	13.6	3.6	6776	0.524, 0.471
PVK:TPD:PBD	(FPQ) ₂ Ir(pic-N-O)	8	12.5	4.9	6.0	1.9	4948	0.648, 0.344
PVK:TPD:PBD	(CPQ) ₂ Ir(pic-N-O)	9	12.9	6.1	11.3	3.2	10,620	0.596, 0.401

^a Turn-on voltage (at brightness of 1 cd/m²).

^b Operating voltage at brightness of 1000 cd/m².

^c Maximum luminance and power efficiency.

^d Values collected at a current density of 10 mA/cm².

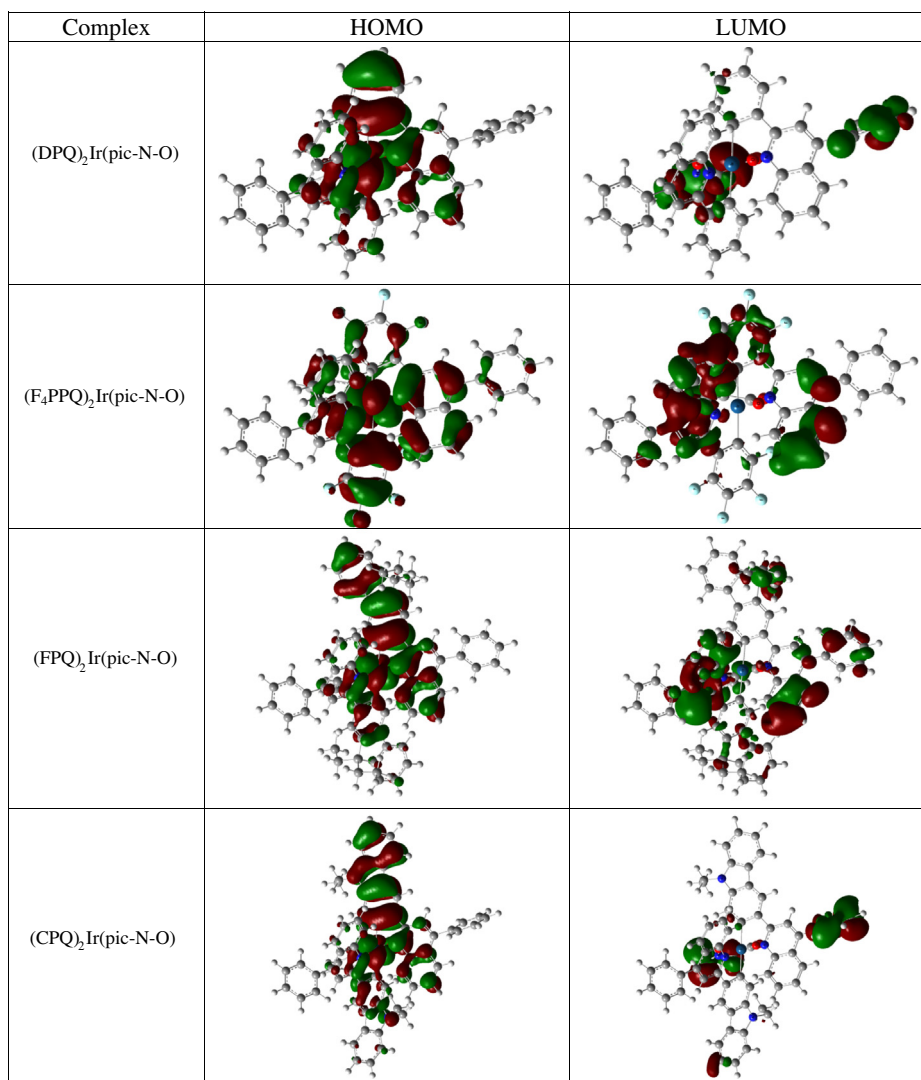


Fig. 9. Calculated HOMOs and LUMOs of Ir(III) complexes.

absorption peaks around 300–400 nm, as calculated absorption peaks often blue-shifted compared to the experimental value.

3. Conclusions

The investigation described above has led to the design and first synthesis of novel, solution processable heteroleptic Ir(III) complexes using various main ligands. We have demonstrated the synthesis of heteroleptic Ir(III) complexes combination of phenylquionlin (PQ) moiety along with phenyl, perfluorinated phenyl, fluorenyl, and carbazolyl groups as a main ligands and pic-N-O ancillary ligand for the fabrication of solution-processed PhOLEDs. Among them, (DPQ)₂Ir(pic-N-O) doped CBP host emission layer gave a high LE of 26.9 cd/A corresponding to an EQE of 14.2%. The overall result showed that although the device performance has not been fully optimized yet, the combination of high efficiency and solution processability

of PhOLEDs that employ these Ir(III) complexes makes them promising candidates for use in light emitting diode devices. Analysis of HOMOs and LUMOs indicate that the electronic excitation (transition) is attributed to MLCT for (F₄PPQ)₂Ir(pic-N-O) and (FPQ)₂Ir(pic-N-O) and LLCT for (DPQ)₂Ir(pic-N-O) and (CPQ)₂Ir(pic-N-O).

4. Experimental

4.1. General Information

All chemicals and reagents were purchased from Aldrich Chemical Co. and used without further purification. The THF solvent was dried and purified by distillation over sodium/benzophenone under nitrogen atmosphere while other solvents were used without additional purification. The ¹H and ¹³C NMR spectra were recorded on a Varian Mercury Plus 300 MHz spectrometer in CDCl₃ using tetramethylsilane as an internal reference. High-resolution

mass spectra data were obtained from the Korea Basic Science and Institute Daejeon Center (HR-ESI Mass). The UV–visible and the fluorescence spectra were recorded on a JASCO V-570 and Hitachi F-4500 fluorescence spectrophotometers at room temperature. Thermal analyses were carried out on a Mettler Toledo TGA/SDTA 851e, DSC 822e analyzer under N₂ atmosphere at a heating rate of 10 °C/min. Cyclic voltammetry (CV) studies were carried out with a CHI 600C potentiostat (CH Instruments) at a scan rate of 100 mV/s in a 0.1 M solution of tetra-*n*-butylammonium hexafluorophosphate (TBAPF₆) in anhydrous acetonitrile/benzene (1:1.5 v/v). A platinum wire was used as the counter electrode and an Ag/AgNO₃ electrode was used as the reference electrode. All of the electrochemical experimental studies were carried out in the open air at room temperature.

4.2. Synthesis of main ligands [DPQ, F₄PPQ, FPQ]

A mixture of starting (1, 4 and 7) (10 mL, 81.9 mmol), 2-aminobenzophenone (18 g, 90 mmol), diphenyl phosphate (DPP, 24.5 g, 98.28 mmol), and *m*-cresol (25 mL) was flushed with nitrogen while stirring at room temperature for 30 min, and then refluxed for 12 h at 140 °C. The reaction mixture was neutralized into 10% sodium hydroxide. The crude mixture filtered through silica gel to remove by-product and unreacted starting material, and then recrystallized from a methylene chloride/hexane.

4.3. Synthesis of [(2,4-diphenylquinoline)₂iridium(III) picolinic acid N-oxide [(DPQ)₂Ir(pic-N-O)]

The cyclometalated Ir(III)-chlorobridge dimer was synthesized by the method reported by Nonoyama [36]. The 2,4-diphenylquinoline (DPQ) (9 g, 32 mmol) and IrCl₃·H₂O (4.6 g, 12.8 mmol) were added to a mixture of 2-ethoxyethanol and water (300 mL, 3:1 v/v). The reaction mixture was stirred at 140 °C for 24 h and a red precipitate was obtained after cooling to room temperature. The precipitate was collected and washed with deionized water (300 mL) and methanol (150 mL). Subsequently, the cyclometalated iridium dimer was dried under vacuum to afford a red solid. Cyclometalated iridium dimer (10.7 g, 7 mmol) and picolinic acid N-oxide (5 g, 35 mmol) were mixed with Na₂CO₃ (7.34 g, 70 mmol) in 2-ethoxyethanol (300 mL). The mixture was refluxed for 12 h under a nitrogen atmosphere. After cooling to room temperature, the crude solution was poured into water and extracted with ethyl acetate, dried over anhydrous MgSO₄ and evaporated by vacuum. The residue was purified by silica gel chromatography (ethyl acetate:hexane:methylene chloride = 1:2:4) as an eluent and additional purified by recrystallization using dichloromethane/ethanol mixture to afford a red solid complex. (3.5 g, 64%)

Anal. Calcd. For C₄₈H₃₂IrN₃O₃: C 64.70, H 3.62, N 4.22; found: C 62.76, H 3.72, N 3.96. HRESI-MS [M + H]⁺: *m/z* found 891.38, calcd for 891.21.

Other Ir(III) complexes, (F₄PPQ)₂Ir(pic-N-O), (FPQ)₂Ir(pic-N-O), (CPQ)₂Ir(pic-N-O) were also prepared from the different main ligands and same ancillary ligand by similar procedure.

[4-Phenyl-2-(2,3,4,5-tetrafluorophenyl)quinoline]₂Ir(III) picolinic acid N-oxide (F₄PPQ)₂Ir(pic-N-O): Anal. Calcd. For C₄₈H₂₄F₈IrN₃O₃: C 55.71, H 2.34, N 4.06; found: C 54.03, H 2.38, N 4.22. HRESI-MS [M + H]⁺: *m/z* found 1035.31, calcd for 1035.13.

[2-(9,9-Diethyl-9H-fluoren-2-yl)-4-phenylquinoline]₂Ir(III) picolinic acid N-oxide (FPQ)₂Ir(pic-N-O): Anal. Calcd. For C₇₀H₅₆IrN₃O₃: C 71.28, H 4.79, N 3.56; found: C 68.42, H 5.02, N 3.45. HRESI-MS [M + H]⁺: *m/z* found 1179.71, calcd for 1179.40.

4.4. Device fabrication and measurements

The indium tin oxide (ITO) glass substrate with a sheet resistance of 20 Ω/square was washed sequentially with a substrate cleaning detergent (Sigma–Aldrich, Micro-90[®] concentrated cleaning solution), deionized water, acetone, and isopropyl alcohol in ultrasonic bath at 50 °C. Prior to spin coating with the PEDOT:PSS layer, the ITO was pre-cleaned and UV–ozone treated. Then a 40 nm-thick PEDOT:PSS (H.C.Starck, Clevios P VP Al 4083) layer was spin coated onto the ITO and baked in a nitrogen environment at 120 °C for 20 min. The EML is consisted of 2-(4-biphenyl)-5-(4-*tert*-butylphenyl)-1,3,4-oxadiazole (PBD), *N,N'*-diphenyl-*N,N'*-bis(3-methyl-phenyl)-[1,1'-biphenyl]-4,4'-diamine (TPD) and either of 4,4'-bis(9-cabazolyl)-biphenyl (CBP) or poly(*N*-vinylcarbazole) (PVK) as a mixed host and Ir(III) complex as a dopant. The blending ratio of CBP (or PVK), TPD and PBD is 56:12:24 wt%, respectively, and doped with 8 wt% of Ir(III) complex in chlorobenzene solution. The EML was obtained by spin coating onto the PEDOT:PSS layer and annealed at 70 °C for 30 min in highly pure argon filled glove box in order to get thickness of 70 nm. Bphen (20 nm) as an electron transport layer as well as hole blocking layer, LiF (0.7 nm) and Al (100 nm) as typical cathode were evaporated under the vacuum less than 6 × 10⁻⁶ torr, which yielded a 9 mm² of emitting area for each pixel. Each layer of thickness was measured by an Alpha-step IQ surface profiler (KLA Tencor, San Jose, CA). The EL spectra and CIE coordinates were measured using a PR650 spectra colorimeter. To characterize the PhOLEDs, the *J*–*V*–*L* changes were measured using a current/voltage source meter (Keithley 236) and an optical power meter (CS-1000, LS-100). All processes and measurements were carried out in the open air at room temperature.

Acknowledgments

This work was supported by a grant funds from the National Research Foundation of Korea (NRF) of the Ministry of Education, Science and Technology (MEST) of Korea (No. 2011-0028320). LD and JL thank AFOSR (FA9550-12-1-0069) for partial support.

Appendix A. Supplementary material

Supplementary data associated with this article can be found, in the online version, at <http://dx.doi.org/10.1016/j.orgel.2013.05.013>.

References

- [1] C.H. Chien, C.K. Chen, F.M. Hsu, C.F. Shu, P.T. Chou, C.H. Lai, Multifunctional deep-blue emitter comprising an anthracene core and terminal triphenylphosphine oxide groups, *Adv. Funct. Mater.* 19 (2009) 560–566.
- [2] X. Xing, L. Zhang, R. Liu, S. Li, B. Qu, Z. Chen, W. Sun, L. Xiao, Q. Gong, A deep-blue emitter with electron transporting property to improve charge balance for organic light-emitting device, *ACS Appl. Mater. Interf.* 4 (2012) 2877–2880.
- [3] L. Xiao, Z. Chen, B. Qu, J. Luo, S. Kong, Q. Gong, J. Kido, Recent progresses on materials for electrophosphorescent organic light-emitting devices, *Adv. Mater.* 23 (2011) 926–952.
- [4] R. Ragni, E. Plummer, K. Brunner, J.W. Hofstraat, F. Babudri, G.M. Farinola, F. Naso, L. De Cola, Blue emitting iridium complexes: synthesis, photophysics and phosphorescent devices, *J. Mater. Chem.* 16 (2006) 1161–1170.
- [5] H.J. Bolink, E. Coronado, S.G. Santamaria, M. Sessolo, N. Evans, C. Klein, E. Baranoff, K. Kalyanasundaram, M. Grätzel, Md.K. Nazeeruddin, Highly phosphorescent perfect green emitting iridium(III) complex for application in OLEDs, *Chem. Commun.* (2007) 3276–3278.
- [6] P. Coppo, E.A. Plummer, L. De Cola, Tuning iridium(III) phenylpyridine complexes in the “almost blue” region, *Chem. Commun.* (2004) 1774–1775.
- [7] T. Sajoto, P.I. Djurovich, A.B. Tamayo, M. Yousufuddin, R. Bau, M.E. Thompson, R.J. Holmes, S.R. Forrest, Blue and near-UV phosphorescence from iridium complexes with cyclometalated pyrazolyl or n-heterocyclic carbene ligands, *Inorg. Chem.* 44 (2005) 7992–8003.
- [8] C. Yang, X. Zhang, H. You, L. Zhu, L. Chen, L. Zhu, Y. Tao, D. Ma, Z. Shuai, J. Qin, Tuning the energy level and photophysical and electroluminescent properties of heavy metal complexes by controlling the ligation of the metal with the carbon of the carbazole unit, *Adv. Funct. Mater.* 17 (2007) 651–661.
- [9] R.N. Bera, N. Cumpstey, P.L. Burn, I.D.W. Samuel, highly branched phosphorescent dendrimers for efficient solution-processed organic light-emitting diodes, *Adv. Funct. Mater.* 17 (2007) 1149–1152.
- [10] P. Wellmann, M. Hofmann, O. Zeika, A. Werner, J. Birnstock, R. Meerheim, G.F. He, K. Walzer, M. Pfeiffer, K. Leo, High-efficiency p-i-n organic light-emitting diodes with long lifetime, *J. Soc. Inf. Display* 13 (2005) 393–397.
- [11] M. Cai, T. Xiao, E. Hellerich, Y. Chen, R.J. Shinar, High-efficiency solution-processed small molecule electrophosphorescent organic light-emitting diodes, *Adv. Mater.* 23 (2011) 3590–3596.
- [12] S. Ye, Y. Liu, K. Lu, W. Wu, C. Du, Y. Liu, H. Liu, T. Wu, G. Yu, An alternative approach to constructing solution processable multifunctional materials: their structure, properties, and application in high-performance organic light-emitting diodes, *Adv. Funct. Mater.* 20 (2010) 3125–3135.
- [13] E. Ahmed, T. Earmme, S.A. Jenekhe, New solution-processable electron transport materials for highly efficient blue phosphorescent OLEDs, *Adv. Funct. Mater.* 21 (2011) 3889–3899.
- [14] Y. Yang, Y. Zhou, Q. He, C. Yang, F. Bai, Y. Li, Solution-processable red-emission organic materials containing triphenylamine and benzothiadiazole units: synthesis and applications in organic light-emitting diodes, *J. Phys. Chem. B* 113 (2009) 7745–7752.
- [15] S. Feng, L. Duan, L. Hou, J. Qiao, D. Zhang, G. Dong, L. Wang, Y.A. Qiu, A comparison study of the organic small molecular thin films prepared by solution process and vacuum deposition: roughness, hydrophilicity, absorption, photoluminescence, density, mobility, and electroluminescence, *J. Phys. Chem. C* 115 (2011) 14278–14284.
- [16] X.H. Yang, F.I. Wu, D. Neher, C.H. Chien, C.F. Shu, Efficient red-emitting electrophosphorescent polymers, *Chem. Mater.* 20 (2008) 1629–1635.
- [17] Y.J. Pu, M. Higashidate, K.I. Nakayama, J. Kido, Solution-processable organic fluorescent dyes for multicolor emission in organic light emitting diodes, *J. Mater. Chem.* 18 (2008) 4183–4188.
- [18] S.C. Lo, G.J. Richards, J.P.I. Markham, E.B. Namdas, S. Sharma, P.L. Burn, I.D.W. Samuel, A light-blue phosphorescent dendrimer for efficient solution-processed light-emitting diodes, *Adv. Funct. Mater.* 15 (2005) 1451–1458.
- [19] R.H. Friend, R.W. Gymer, A.B. Holmes, J.H. Burroughes, R.N. Marks, C. Taliani, D.D.C. Bradley, D.A. Dos Santos, J.L. Brédas, M. Lögdlund, W.R. Salaneck, Electroluminescence in conjugated polymers, *Nature* 397 (1999) 121–128.
- [20] T. Guo, R. Guan, J. Zou, J. Liu, L. Ying, W. Yang, H. Wu, Y. Cao, Red light-emitting hyperbranched fluorene-alt-carbazole copolymers with an iridium complex as the core, *Polym. Chem.* 2 (2011) 2193–2203.
- [21] J. Ding, J. Lü, Y. Cheng, Z. Xie, L. Wang, X. Jing, F. Wang, A divergent synthesis of very large polyphenylene dendrimers with iridium(III) cores: molecular size effect on the performance of phosphorescent organic light-emitting diodes, *Adv. Funct. Mater.* 18 (2008) 2754–2762.
- [22] B. Liang, L. Wang, Y. Xu, H. Shi, Y. Cao, High-efficiency red phosphorescent iridium dendrimers with charge-transporting dendrons: synthesis and electroluminescent properties, *Adv. Funct. Mater.* 17 (2007) 3580–3589.
- [23] G. Zhou, W.Y. Wong, B. Yao, Z. Xie, L. Wang, Triphenylamine-Dendronized pure red iridium phosphors with superior OLED efficiency/color purity trade-offs, *Angew. Chem. Int. Ed.* 46 (2007) 1149–1151.
- [24] S.C. Lo, R.E. Harding, E. Brightman, P.L. Burn, I.D.W. Samuel, The development of phenylethylene dendrons for blue phosphorescent emitters, *J. Mater. Chem.* 19 (2009) 3213–3227.
- [25] X. Yang, D.C. Müller, D. Neher, K. Meerholz, *Adv. Mater.* 18 (2006) 948–954.
- [26] K.S. Yook, J.Y. Lee, Solution processed multilayer deep blue and white phosphorescent organic light-emitting diodes using an alcohol soluble bipolar host and phosphorescent dopant materials, *J. Mater. Chem.* 22 (2012) 14546–14550.
- [27] S.J. Lee, J.S. Park, M. Song, I.A. Shin, Y.I. Kim, J.W. Lee, J.W. Kang, Y.S. Gal, S. Kang, Y. Lee, S.H. Jung, H.S. Kim, M.Y. Chae, S.H. Jin, Synthesis and characterization of red-emitting iridium(III) complexes for solution-processable phosphorescent organic light-emitting diodes, *Adv. Funct. Mater.* 19 (2009) 2205–2212.
- [28] A.K. Agrawal, S.A. Jenekhe, Thin-film processing and optical properties of conjugated rigid-rod polyquinolines for nonlinear optical applications, *Chem. Mater.* 4 (1992) 95–104.
- [29] S.J. Lee, J.S. Park, K.J. Yoon, S.H. Jim, S.K. Kang, Y.S. Gal, S. Kang, J.Y. Lee, J.W. Kang, S.H. Lee, H.D. Park, J.J. Kim, High-efficiency deep-blue light-emitting diodes based on phenylquinoline/carbazole-based compounds, *Adv. Funct. Mater.* 18 (2008) 3922–3930.
- [30] S. Lamansky, P. Djurovich, D. Murphy, F. Abdel-Razzaq, R. Kwong, I. Tsyba, M. Bortz, B. Mui, R. Bau, M.E. Thompson, Synthesis and characterization of phosphorescent cyclometalated iridium complexes, *Inorg. Chem.* 40 (2001) 1704–1711.
- [31] H. Razaftirimo, Y. Cao, W.A. Feld, B.R. Hsieh, A layer-wise topographic study of a polymeric light-emitting diode: indium-tin oxide/poly (2,3-diphenyl-p-phenylene vinylene)/Ag, *Synth. Met.* 79 (1996) 103–106.
- [32] C. Liu, X.C. Zou, S. Yin, W.X. Zhang, Influence of spin methods on the performance of polymer light-emitting devices, *Thin Solid Films* 466 (2004) 279–284.
- [33] H.A. Al-Attar, A.P. Monkman, Solution processed multilayer polymer light-emitting diodes based on different molecular weight host, *J. Appl. Phys.* 109 (2011) 074516.
- [34] Q.X. Tong, S.L. Lai, M.Y. Chan, K.H. Lai, J.X. Tang, H.L. Kwong, C.S. Lee, S.T. Lee, Efficient green organic light-emitting devices with a nondoped dual-functional electroluminescent material, *Appl. Phys. Lett.* 91 (2007) 153504.
- [35] M.J. Frisch et al., Gaussian 09, Revision B.01; Gaussian Inc.: Wallingford, CT, 2010.
- [36] M. Nonoyama, Chelating C-metallation of N-phenylpyrazole with rhodium(III) and iridium(III), *J. Organomet. Chem.* 86 (1975) 263–267.